



HAL
open science

Numerical investigation of shear zones in granular materials

Jean Jacques Moreau

► **To cite this version:**

Jean Jacques Moreau. Numerical investigation of shear zones in granular materials. HLRZ-Workshop on Friction, Arching, Contact Dynamics, 1997, Singapour, Singapore. pp.233-247. hal-01825188

HAL Id: hal-01825188

<https://hal.archives-ouvertes.fr/hal-01825188>

Submitted on 28 Jun 2018

HAL is a multi-disciplinary open access archive for the deposit and dissemination of scientific research documents, whether they are published or not. The documents may come from teaching and research institutions in France or abroad, or from public or private research centers.

L'archive ouverte pluridisciplinaire **HAL**, est destinée au dépôt et à la diffusion de documents scientifiques de niveau recherche, publiés ou non, émanant des établissements d'enseignement et de recherche français ou étrangers, des laboratoires publics ou privés.

NUMERICAL INVESTIGATION OF SHEAR ZONES IN GRANULAR MATERIALS

J.J. MOREAU

Laboratoire de Mécanique et Génie Civil,
case 048, Université Montpellier II,
34095 Montpellier Cedex 5, France

Abstract

The Contact Dynamics method is a numerical technique for computing the dynamical motion of collections of bodies submitted to the unilateral constraints of mutual non-interpenetrability, taking into account dry friction in the case of contact and also the velocity jumps which may arise from collisions. The essential nonsmoothness of the problem is faced without resorting to any regularizing approximation such as artificial repulsion or artificial viscosity. The method is illustrated here by the simulation of a rectilinear shear zone occurring in a slowly strained granulate. The concept of Internal Moment is introduced in order to analyse the transmission of forces.

1 Introduction

1.1 Computation in Multibody Dynamics

After the pioneering work of P.A. Cundall [1], a number of authors have developed codes for computing the motion or the equilibrium of collections of bodies through the approximate replacement of the non-interpenetrability constraints by repulsion laws which enter into action when a pair of bodies come sufficiently close to each other. This is the mechanical analogue of the *penalty methods* commonly used in Constrained Optimization. Some of these codes are directly inspired by the numerical techniques of Molecular Dynamics.

Significant simulations of geological structures, of masonry works or of granular materials have been obtained in this way. The main drawback is that the need of precision calls for very stiff repulsion laws, so that the time-discretization algorithms (usually of the explicit type), applied in integrating the equations of Dynamics, have to resort to fine time-steps and possibly also to artificial damping in order to secure numerical stability. In some instances the effects of artificial elastic repulsion and of artificial damping may become difficult to distinguish from those of the mechanically intentional elasticity or damping.

A different class of numerical methods are qualified as *event-driven*. They consist in applying to the unilateral constraints of non-interpenetrability (usually subject to friction) the theoretical procedures of Rational Mechanics. The

second order differential equations of Dynamics are exploited with account of the contact constraints, if some of them are effective during the concerned time interval, and of the associated contact forces. Standard numerical techniques are applied to these equations, allowing one to determine instants at which the status of constraints changes. Such a change may arise from a collision suddenly introducing new constraints, in which case some empirical *collision laws* are invoked in order to determine the new velocities from which the subsequent motion have to be computed. The status of constraints may also change from the *cessation of contacts*, at instants which have to be detected by calculating the contact forces in every contact point. If at some instant a contact force is found with a direction incompatible with unilaterality, one concludes that the further motion has to be calculated by assuming a different set of effective contacts. But it has long been known [2] that the contacts which cease at the detected instant are not necessarily those for which an unfeasible reaction force was calculated. The heart of the matter is a *Complementarity Problem* of the sort commonly met in Convex Optimization [3].

For the application of the above approach to the Dynamics of Machines, which involves a relatively small number of bodies, the reader may refer to [4]. In what concerns Granular Materials, event-driven methods are primarily applied to the dynamics of *dilute states*, so that the interaction of grains solely rests on collisions. A trick to approximate durable contact by motions of this sort consists in introducing some auxiliary agitation. Anyway, event-driven computation becomes unfeasible when the average time between collision is too small.

1.2 The Contact Dynamics Method

This method, abbreviatively labelled as ‘the CD method’ originated in [5], a text in which the unilateral mechanical constraint of (possibly frictional) non-interpenetrability receives a formulation, resting on a theoretical background of elementary Convex Analysis, which proves suitable for numerical computation. This formulation also applies to deformable bodies, spatially discretized by Finite Elements [6], with applications in such domains as Geodynamics or the industrial processes of metal forming.

Only mechanical systems with finite number of degrees of freedom will be considered in this lecture. An exposition of the method in this case may be found in [21]. The possibility of collisions makes one expect velocities to be discontinuous functions of time. Actually, in the Dynamics of systems affected with dry friction, velocity jumps may even occur in the absence of any collision as the result of some sort of *dynamic locking* [7].

The mathematical formulation of the corresponding evolution problems rests on the assumption (for which some mechanical justification exists [8]) that velocities are vector functions of time with *locally bounded variation* [9]. Then the role of the accelerations is played by *vector measures* on the considered time interval. In the traditional smooth case, these measures happen to possess density functions relatively to the Lebesgue measure dt , which are nothing else than the accelerations, as functions of time. Possible isolated velocity jumps manifest themselves in this formalism by ‘atoms’ of the above measures, i.e. some vector-valued Dirac measures localized at the corresponding instants. The system dynamics is expressed in general as a *measure differential inclusion* instead

of the conventional differential equation of ‘smooth’ Dynamics.

The analysis of the solutions, i.e. the theoretical study of their existence and of their approximations, is a rather technical matter. The interested reader may refer to [10] for these mathematical aspects, but the principal merit of the formulation lies in its ability to generate time-discretization algorithms which, at every step, are ready to treat velocity jumps on the same footing as smooth evolutions. The discretized equation merely expresses the balance of momentum on the corresponding time-interval, should the involved mechanical actions be ordinary forces or percussions. The nature of the calculations to be effected at each time-step makes the resulting algorithms belong to the *implicit* type, so that they are never hampered by numerical instability.

The physical information concerning the contact interactions is fed into the calculation in a standardized form called a *complete contact law*, devised in order to take care automatically of the geometric conditions of non-interpenetrability. Of course, these contact laws have to encapsulate not only the description of unilaterality and friction in persistent contacts but also the model accepted for predicting the outcome of possible collisions.

At each time-step, an iterative procedure is applied in order to calculate simultaneously all contact impulses, collisional or not, and the resulting changes in velocities. The computation cost of this procedure naturally increases with the number of contacts to be handled. Parallelisation is currently investigated but, up to now, only microcomputers or workstations have been employed. For a dense pack of 4000 round grains, the computation time is typically 15 s per step in two-dimensional situations, 30 s per step in three-dimensional ones, on a Power Macintosh 8500 microcomputer. The detection of contacts is implemented in such a way that it takes only a fraction of a second in the above case. In near-equilibrium situations, computation becomes much quicker because the iterative procedure uses as first guess the contact forces calculated at the preceding step (in particular, if an equilibrium state is attained at a specified precision level, each step only consists of a precision check). Of course, in the collision-dominated dynamics of rapid granular flows, the latter trick has no effect, but in this case speed is favoured by the reduced number of contacts. The choice of the step-length, in order to reach a given precision depends, for compact states on the magnitude of the acting forces and, in rapid flows, on the magnitude of the collision velocities. Of course, quantitative rules could be formulated in the framework of a dimensional inspection. For instance, reducing the acting forces is equivalent to increasing the mass of each grain.

1.3 Collisions

Physically, a collision is a ‘short’ episode during which the contact forces between the involved bodies assume ‘large’ values. The phenomenon cannot be properly analyzed without taking body deformations into account, not only in what concerns the vicinity of the impact locus but also in discussing to what extent some wave-like propagation may transfer momentum to other parts of the investigated system. However, from the beginnings of Mechanics, it has been attempted to incorporate collisions into the dynamical study of bodies though observed at such a scale that microscopic deformations are invisible. This is called the theory of *Rigid Body Collisions*, a recent survey of which may be found in [11]. The objective is to calculate the velocities of the system parts

after the collision from the values these velocities had before it. The ‘collision operators’ commonly used to this end can only provide rather crude predictions, as long as a detailed analysis of the collision process is not made, usually carried out through multiple scaling techniques involving a ‘microtime’. Furthermore, one should keep in mind that if a body engaged in a collision is part of cluster of previously contacting objects, all contact points in the cluster are liable to transmit percussions. In such cases of multiple collisions the traditional concept of restitution coefficient may produce grossly incorrect results.

In CD algorithms, the following improvement on the restitution concept provides a treatment of multiple collisions which at least has the merit of consistency. Contact laws, similar to those applied to persistent contacts, are invoked, in order to connect the (unknown) contact percussions with some formal velocities. The latter are constructed from the (known) pre-collision velocities and from the (unknown) post-collision ones, by a weighted averaging operation. If all the weight is placed on post-collision velocities, the consequent prediction turns out to be that of a collision of the *fully inelastic* sort. On the contrary, by placing equal weights on both velocities, one generates a model of *fully elastic* collision. At each contact point, different weights may be assigned to the tangential and to the normal components of the relative velocities.

The invoked contact laws also include friction. In the simple case of a binary collision, this approach results in a collision operator involving three parameters, identifiable as the *friction coefficient*, the *normal restitution coefficient* and the *tangential restitution coefficient*. For spherical bodies, the resulting formula comes out identical to what has been proposed, from an entirely different background in [12][13], fairly agreeing with the experiments of [[14]].

The computation of the shaking of dense granulates related in [22] provides typical examples of multiple collisions. Physically, one expects that the transmission of collisional impulses throughout a pack of contacting grains involve the elastic deformation of these grains in a process quite similar to the propagation of sound. Since it has been decided here to model grains as perfectly undeformable, such propagative effects are ignored. The success of the method in the investigated instances should be ascribed to the fact that, physically the time taken by sound-like disturbances to travel the extent of the experimental cell is definitely shorter than the period of shake.

In contrast, multiple collisions play a minor role in the dynamics of dilute granulates. The greater efficiency of the CD method, if compared with event-driven ones, mainly stems from that, once a time-discretization mesh has been chosen, all the collisions which are detected as occurring on a given time-step are treated together. This of course entails some trade-offs which have to be assessed. It seems of little consequence that the ordering of the collisions, which mechanically should be successive, is only internal to the algorithm. In fact, the problems in view are physically undeterministic, since a slight change in the initial conditions is enough to produce, after a short time, a completely different sequence of positions and collisions. A more critical observation is that each collision is treated as occurring only once between the involved bodies in the considered time-step. An accumulation of bounces, such as those of a ping-pong ball coming to rest, is thus viewed as a single collision as soon as the expected successive bounces are all comprised in the same time-step. This could result in underestimating the energy loss arising from inelastic collisions. This source of error may be checked by repeating the computation with reduced

time step : if no change is found in the energy vs time curve, one may conclude that no harm was done.

1.4 Previous Applications of the Method

Calculations of shaken granular materials, in two or three dimensions, have been the first published illustrations of the CD method. They gave the occasion of very convincing comparisons [21] with the physical experiments related in [23], evidencing the effects of boundary friction : boundary vortices and heaping.

Concerning the popular phenomenon of *size-segregation* the role, in certain settings, of the friction-induced boundary currents and the consequent convection effects has been revealed [20], independently of the experiments of [24]. Furthermore, CD simulation has disclosed how such boundary currents are generated.[22]

Above applications pertained to the rapid dynamics of dense granular materials. Actually, some simulations of slow deformation have confirmed that, even if the external driving which compels a granular sample to deform is so slow that, at the level of the overall motion, acceleration effects seem negligible, this is not usually the case microscopically.[25] It is well known (see, in particular [19]) that the deformation involves a succession of *crises* which essentially are dynamical processes. Consequently, in numerical simulations, the grain masses must be entered with their true physical values, without attempting to improve computation speed by artificially increasing them.

Provided dynamical effects are taken into account, the average stress due to contact in a portion of deforming granulate remains a meaningful element of the analysis. We therefore have to revisit this concept before finally presenting in Sec.3 below a detailed example of shear.

2 The Definition of Stress

A number of authors have proposed definitions of the stress in a portion of granular material in equilibrium or quasi-equilibrium, all essentially equivalent [see, among others, [27] [28] [29]]. If dynamical effects are also to be taken into account, one should first recall that the convection of momentum significantly contributes to the transmission of macroscopic efforts in the standard kinetic theory of fluids as well as in the modelling of dilute granular flows [see e.g. [30]]. But, in the evolution of dense granulates which is the subject of this lecture, the mean free path appears negligible in regard to particle size. Consequently, a concept pertaining only to *contact* interactions, possibly collisional, is all what is needed. Anyway, the following [31] remains consistent in all situations.

By a *fragmented system*, we mean a collection of (deformable or rigid) bodies which interact only through contact. Examples: a granular material, a piece of masonry. In order to define, for such a system, some concept able to play, as far as possible, the role that the Cauchy stress tensor holds in conventional continuous media, we are to introduce the ‘internal moment tensor’ of an arbitrary material system. This does not require of the number of constituents to be large and the concept makes sense even for a single granule. In particular, when constructing averages over a granular sample, one may also investigate the statistical dispersion of the individual terms involved.

2.1 The Virtual Power Formalism

According to this standard formalism of Classical Mechanics,[32] any *effort* (this is not necessarily a force in the traditional sense) experienced by a material system is defined by the expression of the power that this effort would develop if the system elements were affected by a class of imagined velocity fields, called *virtual velocities* or *test fields*. The rule of the game is that this class of vector fields constitutes a linear space and that the functional ‘power’ is linear on this space.

Let S be a material system occupying a bounded portion of space and let φ denote an affine test field, with Cartesian components

$$\varphi_i(x) = \varphi_i(o) + b_{ij}x_j. \quad (1)$$

Since the power $P_{\text{int}}(S, \varphi)$ of the *internal efforts* of S when φ is taken as test field depends linearly on φ , i.e. linearly on the parameters $\varphi_i(o)$ and b_{ij} , there exist R_i and M_{ij} such that $P_{\text{int}}(S, \varphi) = R_i\varphi_i(o) + M_{ij}b_{ji}$.

The virtual power formalism generalizes Newton’s third law in the form:

The internal efforts of any material system have zero power whenever φ equals the velocity field of a rigid motion, i.e. a field as in Eq.(1) with $b_{ji} = -b_{ij}$ (provided Cartesian coordinates are orthonormal).

This readily implies that R_i vanishes and that M_{ij} constitutes the components of a symmetric tensor M of rank 2, independent of the choice of the origin and of the (orthonormal) axes in use. Let us call this tensor the *Internal Moment* of S .

Example. Let S consist of a portion of a classical continuous medium occupying a bounded domain Ω of space, with σ as Cauchy stress field. Then classically, for every continuously differentiable φ ,

$$P_{\text{int}}(S, \varphi) = \int_{\Omega} \sigma_{ji}\varphi_{i,j} d\omega. \quad (2)$$

This actually constitutes the very definition of the Cauchy stress in a synthetic construction of Continuum Mechanics [32].

Here we comply with the common usage in Geomechanics and Civil Engineering of counting a stress as *positive* when it is directed as a *pressure*. In Mechanical Engineering and in general Continuum Mechanics, the reverse convention is applied, which would require a *minus* sign in the right-hand side of Eq.(2).

By taking as φ the same affine vector field as before, one obtains

$$M_{ij}(S) = \int_{\Omega} \sigma_{ij} d\omega. \quad (3)$$

2.2 The Static Case

Assume in this Subsec. that the considered system is in *equilibrium*. Then the *Principle of Virtual Power* states that the total power of all the efforts it experiences, namely the internal and the external ones, equals zero whatever is φ , so $P_{\text{int}} = -P_{\text{ext}}$. If, for instance, the external efforts experienced by S simply

consist of a finite collection of forces f^α exerted at points x^α , one may take φ as in Eq.1 and find

$$M_{ij} = - \sum_{\alpha} x_i^\alpha f_j^\alpha \quad (4)$$

i.e. in the event of equilibrium, the internal moment equals the opposite of the moment tensor of the external forces. The latter is by itself independent of the choice of the origin and symmetric because the equations of Statics make the resultant of external forces vanish, as well as their skew moment. All the above writing readily extends to continuously distributed external efforts, such as gravity forces, and also to external efforts of *higher order*. The latter may include space distributions of magnetic actions or the boundary couples commonly introduced in the phenomenological description of the resistance to rolling, but this does not prevent M from being a *symmetric* tensor of rank 2.

2.3 Additivity

Suppose that S equals a collection of subsystems S_1, S_2, \dots *which interact only through contact actions*. The internal efforts of S consist of the respective internal efforts of the subsystems and of the mutual efforts that these subsystems may exert upon each other. Since the efforts exerted, say by S_1 upon S_2 and by S_2 upon S_1 are contact actions (possibly involving couples of resistance to rolling), they are located at the same points of space and, by Newton's third law, have opposite values. Therefore, the total contribution of these mutual efforts in the internal moment of S vanish, so one has $M(S) = M(S_1) + M(S_2) + \dots$

More generally, by assigning to every finite collection of subsystems of S the corresponding internal moment, one defines a *finitely additive tensor-valued measure*.

The occurrence of an integral in Eq.(3) makes additivity evident in this special case and shows that, in a classical continuous medium, the Cauchy stress field is nothing else than the *density function* of the internal moment measure relatively to the volume (i.e. Lebesgue) measure. The same equation expresses that the *volume average* of the Cauchy stress field over Ω equals $M/\text{vol}(\Omega)$.

Therefore, if a portion S of granular material is viewed as 'enveloped' in a bounded domain Ω , it is natural to say that the tensor $M(S)/\text{vol}(\Omega)$ constitutes the *average stress* of S . The uncertainty in defining such an enveloping domain has little consequence if S is sufficiently dense and comprises sufficiently many grains. It is only at this stage that some assumption of 'large number' has to be made. It will be shown on the example of Sec.3 that the tensor calculated in that way does possess the main property expected of the Cauchy stress, namely it allows one to predict how the force transmitted across an ideal cut depends on the direction of this cut.

The above construction, based on the Virtual Power formalism, has the advantage of possible extension to many other models of continuous media. For instance the internal moment measure of a *string* or a *chain* admits a density function relatively to the arc-length measure. The visualisation of *force chains* in the granular sample of Sec.3 through the internal moments of individual grains suggests that the construction of models of granular media could rest on formulations in which the internal moment measure would not be represented by a density with respect to volume.

2.4 The Dynamical Terms

The existence of the tensor $M(S)$ and its additivity property for a fragmented material system are inherent in the principles of Classical Mechanics. There only remains to know how to evaluate this tensor in specific situations.

Equation (4) pertains to the special case of equilibrium. If, more generally, the motion of S relative to some *inertial* reference frame, under some specified mechanical actions, has been calculated, one has to express that, for every test field φ , the virtual power of all the efforts experienced by the system equals that of the vector measure $a(x) d\mu(x)$, where a denotes the acceleration field and μ the mass measure. By using as φ the same affine vector field as before, one obtains, for every fragment s of the system, in coordinate-free notation,

$$M(s) = -\text{tens.mom}(\text{ext.efforts}) + \int_s x \otimes a(x) d\mu(x). \quad (5)$$

This applies, in particular, to each element of a granulate material. The total expression on the right-hand side, like $M(s)$ itself, does not depend on the choice of the origin. When s is an indeformable grain, it proves convenient to take as origin the center of mass of this rigid body, then express $a(x)$ by the standard formulas of rigid body kinematics and use the inertia tensor of s in order to calculate the integral in closed form. The result involves in general the acceleration of the center of mass of s , the spin vector ω and its time-derivative ω' .

Let us only report the simplification which occurs in two-dimensional situations, when the rigid grain possesses *rotational symmetry*. Then Eq.(5) is found to reduce to

$$M(s) = -\text{sym.mom}(\text{ext.efforts}) - \frac{1}{2} \omega^2 I \mathbf{1}. \quad (6)$$

where I denotes the moment of inertia of s about its center and $\mathbf{1}$ the rank 2 unit tensor. The symmetric moment tensor of external efforts is evaluated about the center of s . Interestingly, ω' does not appear in this special case.

What precedes readily adapts to instants at which efforts are of percussional nature. Recall in this connection that CD computation consists in solving, on each time-step, the balance of momentum of the system, in which forces manifest themselves through *impulsions*. Proper forces are retrieved after division by the step-length.

3 Slow Deformations of a Dense Granular Material

Due to space limitation, we restrict ourselves in this paper to the description of a single numerical experiment, concerning a compact two-dimensional assembly of strictly indeformable *circular* objects. Of course, the CD method could as well be applied to some models approaching natural grain shape more closely [16]. The choice of the circular shape is not uniquely motivated by computational ease, but by the want of avoiding the mix of distinct effects. In [17] physical experiments on the slow shear of assemblies of elongated particles are reported. There is shown that shear may induce orientation effects, making of a ‘shear band’ a structurally individualized part of the granulate, strongly affecting in

particular the pattern of force chains. Similarly in [18], the numerical simulation of assemblies of elliptic particles (performed by a method of elastic repulsion) reveals some structural effects of particle elongation during shear.

Let a two-dimensional pack of circular grains be squeezed between two parallel platens with locations $y = y_{\text{inf}}$, $y = y_{\text{sup}}$. In laboratory, the two lateral free boundaries of such a pack would be sustained by the pressure of a liquid, separated from the granulate by a membrane. We rather use here an ideal containing action, easier to analyze. The grains are sorted according to y , so as to divide the height $y_{\text{sup}} - y_{\text{inf}}$ into horizontal bands of uniform width w . In each band the five ending grains on the left are submitted, in proportion to their respective masses, to horizontal forces totalizing wP , where P denotes a fixed pressure. The five ending grains on the right are similarly submitted to horizontal forces totalizing $-wP$. The width w , i.e. the number of bands, is adjusted in order that five grains make sufficient barriers at both ends of each band.

Platen friction is chosen greater than interparticle friction. If platens were forced to move vertically toward each other, this would generate the same classical X-shaped shear as in the simulations related in [26]. Here we instead produce a single straight shear zone which proves more informative. This is done by maintaining the lower platen fixed, while the upper one is given a 45° downward motion. A short time after start, the velocity vectors of the grain centers assume the distribution shown on Fig.1. Nearly undeforming packs look attached to the respective platens, while an oblique shear zone lies in-between.

On Fig.2, a grid of 16 strips, parallel to the general direction of shear, has been superimposed to the zone. For each strip, the average of the longitudinal components of velocities is calculated. The result plotted in the histogram reveals a rather smooth transition from the zero velocity of the lower part to the constant value corresponding to the forced motion of the upper platen. This takes place on a length approximately equal to 25 times the average diameter of grains, but no clear limit can be ascribed to the shear zone.

Incidentally, one can also detect in all regions some grains with aberrant velocities. Through zooming, these grains would be seen flying inside persistent cavities. This is the very effect commonly observed when watching shear-box experiments performed on *Schneebeli materials*, i.e. piles of cylindrical rods stacked parallel. Such grains originate from a partial collapse of the cavity boundary and their velocity of expulsion may be much larger than the velocity of the overall motion. Of course, a free grain ends by hitting the cavity boundary, possibly triggering some rearrangement in the granulate.

Rapidly changing undulations affect the velocity pattern in the shear zone. Sometimes, one may distinguish assemblies of a few grains whose velocity distribution is approximately that of a solid rotation. This reminds one of the persistent rigid clusters observed in real sand experiments.[28] That the effect here is much less pronounced and very fugacious probably comes from the grains being circular. Anyway such swirles have nothing to do with the vortices generated when two fluid flows merge. In the latter case, vortices last sufficiently long for their convection by the fluid to be observed. Furthermore, the velocity distribution in a fluid vortex is quite different, since velocities become larger toward the center.

In Fig.1, three rectangular probing areas have been placed on the field. At the center of each one, a cross represents the principal directions and principal

values of the *average stress tensor*, as defined in Sec.2. For each area, the *histogram of contact normals* is drawn, constructed by dividing the plane into 24 sectors. Each sector is filled in gray up to a radius proportional to the number of the contact points at which the normal n to the contacting grains (in either direction, so that the histogram is symmetric) belongs to the sector. The elongated shapes of these histograms reveal a strong anisotropy in the distribution of contact orientations. The dominant direction may be estimated by constructing the *fabric tensor* relative to the probing area, i.e. the symmetric tensor whose components equal the averages of $n_i n_j$ and determining the major principal direction of this tensor. The table at the top shows that this major principal direction is, in each of the three cases, close to that of the average stress tensor.

The dynamical terms, as expressed in Subsec.2.4, have been taken into account when computing the components of average stress tensors. Actually, they have been found to contribute by less than 0.1 % in the result. The point is that the reported numerical experiment exhibits little dynamical effects. This should be ascribed in part to the relative magnitudes of the upper plate velocity, of the lateral pressure and of the grain masses. The present setting also differs from that of a shear-box by the presence of the lateral free boundaries. Exerting a distributed contention pressure upon these boundaries generates less frustration than acting on the granulate by means of a rigid wall. The global effect of dynamical crises may be assessed by calculating the normal components of the resultant forces exerted by the grains upon the two platens. Since the lateral contention forces are horizontal a difference between these two components purely reflects dynamical effects. In the present experiment the difference remains inferior to 1%, while in the analogous setting of a granulate confined between parallel platens under *periodic* lateral conditions (which are more frustrating than a pressure) the difference may sometimes attain 50%.

The main observation to be made here is that the central oblique probing area, which covers the shear zone and the two other ones covering the vicinity of the platens do not reveal significant differences in average stress and in fabric anisotropy.

On Fig.2, the *force chains* are visualized by drawing the crosses representing the internal moments of all grains individually. Another visualisation of these chains is provided on Fig.3 by representing each pair of intergranular forces by a line segment centered at the contact point. Both representations make clear that *the pattern of force chains is completely indifferent to the presence of the shear zone.*

A circular probing area has been placed in the upper part of the sample on Fig.3. The program has calculated, for a series of diameters, the resultant force exerted by the grains with centers on one side upon those on the other side. The corresponding plot allows one to compare the values with the result of a calculation based on the average stress tensor of the area. In spite of the relatively small number of grains involved for each diameter and of the inhomogeneity due to force chains, the two plots are remarkably concordant.

References

- [1] P.A. Cundall, A computer model for simulating progressive large scale movements of blocky rock systems, *Proceedings of the Symposium of the International Society of Rock Mechanics*, (Nancy, France, 1971), Vol.1, 132-150.
- [2] E. Delassus, Mémoire sur la théorie des liaisons finies unilatérales, *Ann. Sci. Ecole Norm. Sup.*, **34**, 1917, 95-179.
- [3] J.J. Moreau, Quadratic programming in mechanics: dynamics of one-sided constraints, *SIAM J. Control*, **4**, 1966, 153-158.
- [4] F. Pfeiffer & C. Glocker, *Multibody Dynamics with Unilateral Contacts* (John Wiley & Sons, New York, 1996).
- [5] J.J. Moreau, Unilateral contact and dry friction in finite freedom dynamics, in *Nonsmooth Mechanics and Applications*, eds. J.J. Moreau & P.D. Panagiotopoulos (CISM Courses and Lectures, **302**, Springer-Verlag, Wien, New York, 1988), 1-82.
- [6] M. Jean, Frictional contact in collections of rigid or deformable bodies: numerical simulation of geomaterials, in *Mechanics of Geomaterial Interfaces*, eds. A. P. S. Salvadurai & M. J. Boulon, (Elsevier Science Publisher, Amsterdam, 1995) 463-486.
- [7] L. Lecornu, Sur la loi de Coulomb, *Comptes Rendus Acad. Sci. Paris*, **140**, 1905, 847-848.
- [8] J. J. Moreau, An expression of classical dynamics, *Ann. Inst. H. Poincaré Anal. Non Linéaire* **6** (suppl.), 1989, 1-48. Volume also available as *Analyse Non Linéaire*, eds. H. Attouch, J.-P. Aubin, F. Clarke & I. Ekeland (Gauthier-Villars, Paris, 1989).
- [9] J.J. Moreau, Bounded variation in time, in *Topics in Nonsmooth Mechanics*, eds. J.J. Moreau, P.D. Panagiotopoulos & G. Strang (Birkhäuser, Basel, Boston, Berlin, 1988), 1-74.
- [10] M.D.P. Monteiro Marques, *Differential Inclusions in Nonsmooth Mechanical Problems: Shocks and Dry Friction* (Birkhäuser, Basel, Boston, Berlin, 1993).
- [11] B. Brogliato, *Nonsmooth Impact Mechanics. Models, Dynamics and Control* (Lecture Notes in Control and Information Sciences, **220**, Springer-Verlag, 1996).
- [12] O. R. Walton, Numerical simulation of inelastic, frictional particle-particle interactions, in *Particulate two-phase flow*, ed. M. C. Roco (Butterworth-Heinemann, Boston, 1993) 884-910.
- [13] C. K. K. Lun & A. A. Bent, 1993, Computer simulation of simple shear flow of inelastic frictional spheres, in *Powders and grains 93*, ed. C. Thornton (Balkema, Rotterdam, 1993), 301-306.

- [14] S. Foerster, M. Louge, H. Chang & K. Allia, Measurements of the collision properties of small spheres, *Phys. Fluids* **6**, 1994, 1108-1115.
- [15] F. Radjai, M. Jean, J. J. Moreau & S. Roux, Force distributions in dense two-dimensional granular systems, *Phys. Rev. Lett.* **77**, 1996, 274- .
- [16] I. Laalaj, K. Sab & N. Guérin, Micromechanical modelling of ballasted tracks, in *Contact Mechanics*, eds. M. Raous et al. (Plenum Press, New York, 1995), 363-368.
- [17] M. Oda, Micro-fabric and couple-stress in shear bands of granular materials, in *Powders and grains 93*, ed. C. Thornton (Balkema, Rotterdam, 1993), 161-166.
- [18] L. Rothenburg & R.J. Bathurst, Micromechanical features of granular assemblies with planar elliptical particles, *Géotechnique* **42**, 1992, 79-95.
- [19] W. Meftah, P. Evesque, J. Biarez, D. Sornette, & N.E. Abriak, Evidence of local ‘seisms’ of microscopic and macroscopic stress fluctuations during the deformation of packings of grains, in *Powders and grains 93*, ed. C. Thornton (Balkema, Rotterdam, 1993), 173-178.
- [20] J.J. Moreau, New computation methods in granular dynamics, in *Powders and grains 93*, ed. C. Thornton (Balkema, Rotterdam, 1993), 227-232.
- [21] J.J. Moreau, Some numerical methods in multibody dynamics : application to granular materials, *Eur. J. Mech., A/Solids*, **13**, n°4 - suppl., 1994, 93-114.
- [22] J.J. Moreau, Numerical experiments in granular dynamics: vibration-induced size segregation, in *Contact Mechanics*, eds. M. Raous et al. (Plenum Press, New York, 1995), 347-358.
- [23] E. Clément, J. Duran & J. Rajchenbach, Experimental study of heaping in a two-dimensional ”sandpile”, *Phys. Rev. Lett.* **69**, 1992, 1189-1192.
- [24] J.B. Knight, H.M. Jaeger & S.R. Nagel, Vibration-induced size separation in granular media : the convection connection, *Phys. Rev. Lett.* **70**, 1993, 3728-3731.
- [25] M. Jean & J.J. Moreau, Numerical treatment of contact and friction: the Contact Dynamics method, *Proc.1996 Engineering Systems Design and Analysis Conference*, eds. A. Lagarde & M. Raous (Amer. Soc. of Mech. Engineers, New York, 1996), vol.4, 201-208.
- [26] J.P. Bardet & J. Proubet, A numerical investigation of the structure of persistent shear bands in granular media, *Géotechnique* **41**, 1991, 599-613.
- [27] J. Weber, Recherches concernant les contraintes intergranulaires dans les milieux pulvérulents, *Cahiers du Groupe Francais de Rhéologie* **2**, 1966, 161-170 (see also a more detailed account under the same title in *Bulletin de Liaison des Ponts et Chaussées* **20**, jul.-aug. 1966, pp. 3-1 to 3-20).

- [28] A. Drescher & G. De Josselin de Jong, Photoelastic verification of a mechanical model for the flow of a granular material, *J. Mech. Phys. Solids*, **20**, 1972, 337-351.
- [29] L. Rothenburg & R.J. Bathurst, Analytical study of induced anisotropy in idealized granular materials, *Géotechnique* **39**, 1989, 601-614.
- [30] S. B. Savage & D.J. Jeffrey, The stress tensor in a granular flow at high shear rate, *J. Fluid Mech.* **110**, 1981, 255-272.
- [31] J.J. Moreau, Internal moment and contact forces in fragmented materials, oral lecture at *EUROMECH Colloquium 351: Systems with Coulomb Friction*, Vadstena, Sweden, Aug. 5-7, 1996.
- [32] P. Germain, The method of virtual power in continuum mechanics. Part 2: microstructures, *SIAM J. Appl. Math.* **25**, 1973, 556-575.

Granular sample obliquely squeezed between parallel platens

Forced velocity of upper platen : (cm/s) $u = 0.2$, $v = -0.2$. Lower platen fixed.
 Number of grains : 4025. Diameters : uniformly distributed between 0.75 mm and 1.50 mm
 Current height of the sample : 9.34 cm. Grain density : 1 g/cm^3 .
 Intergranular friction : 0.5. Platen friction : 1. Restitution coefficients : 0 everywhere.
 Lateral pressure: 1070 Pa. Gravity neglected.

	Principal stresses (Pascal)		Major principal direction (degrees from horiz. axis)	
	Stress	Fabric	Stress	Fabric
Upper area (1549 points of contact)	2345	1173	+89.6	-88.2
Shear area (2207 points of contact)	2502	1044	-88.6	+89.6
Lower area (1578 points of contact)	2336	1141	+89.2	+88.2

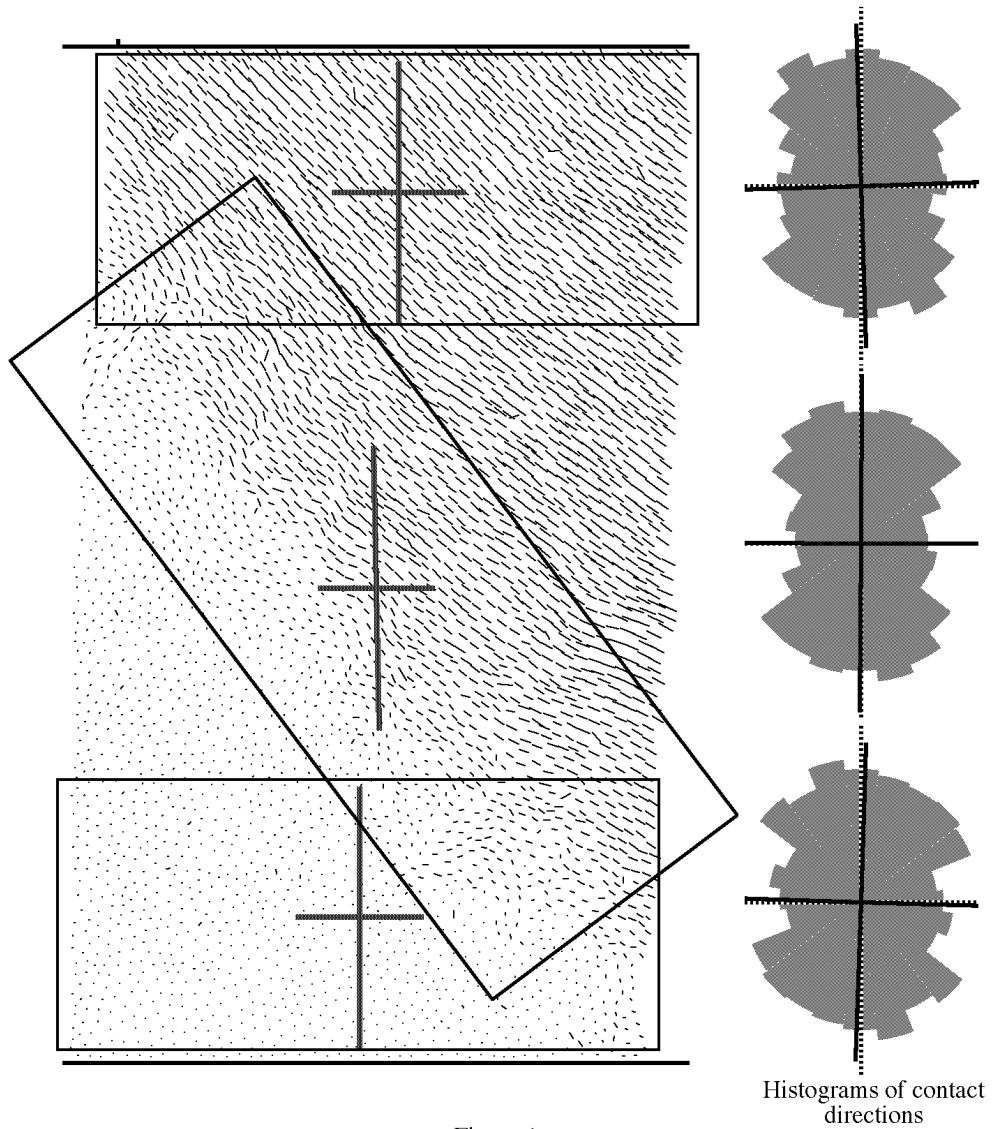


Figure 1

Shear and force chains

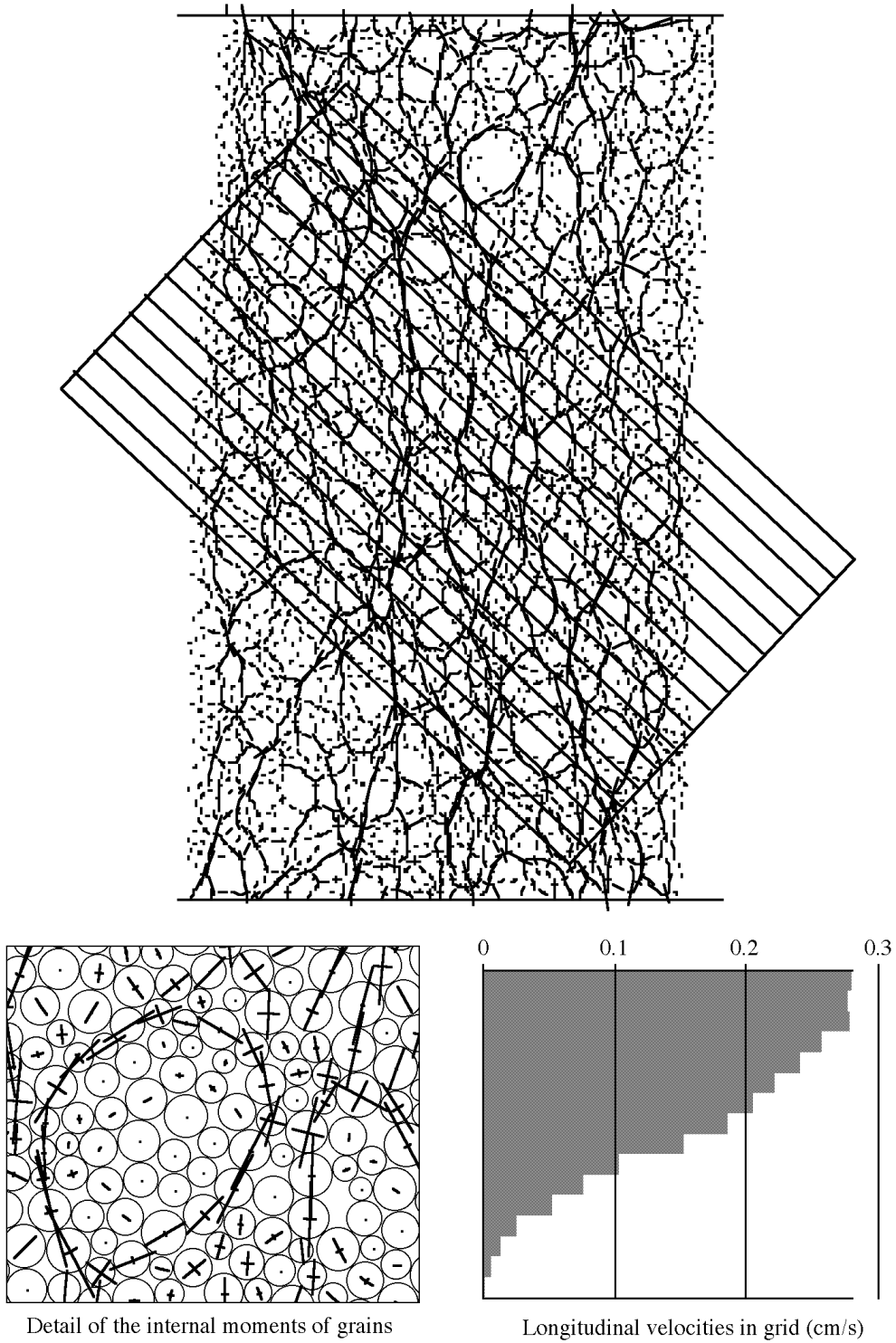
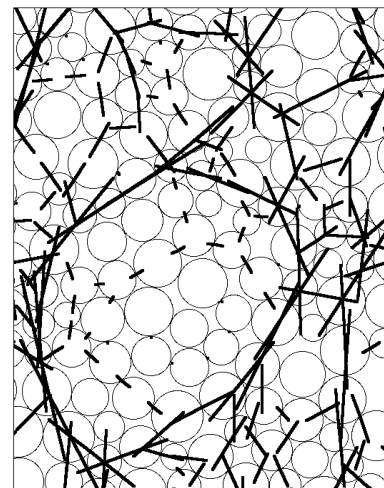
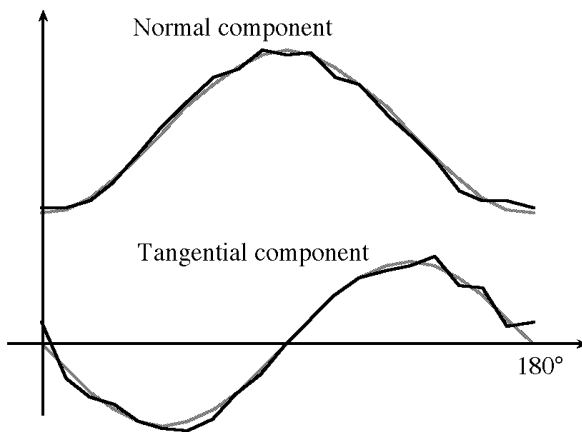
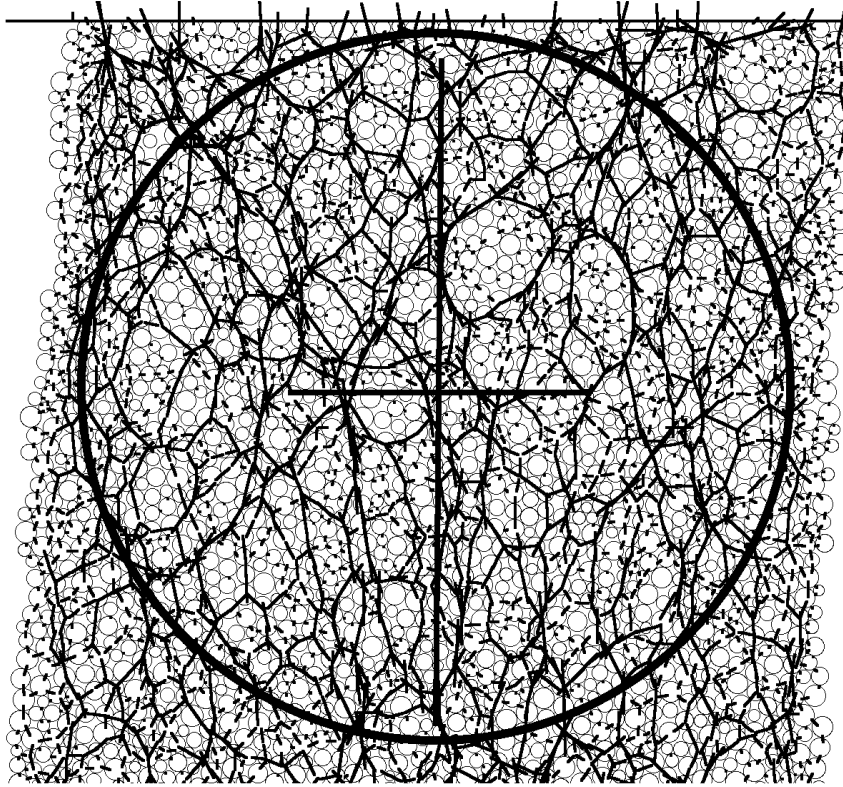


Figure 2

Intergranular forces and average stress tensor

Average stress tensor in circular area. *Principal stresses* : 2600 Pa, 1156 Pa
Direction of major stress : $89^{\circ}.5$ from horizontal axis



Resultant forces across diameters of the circular area
gray curve : *calculated from the average stress*
black curve : *direct analysis of contact forces*

Detail of contact forces

Figure 3